ResearchGate

See discussions, stats, and author profiles for this publication at: https://www.researchgate.net/publication/225092657

Electrochemically Active Dendrimers for the Manufacture of Multilayer Films: Electrochemical Deposition or Polymerization Process by End-Capped Triarylamine or Carbazole Dendrimer

ARTICLE *in* THE JOURNAL OF PHYSICAL CHEMISTRY C · JANUARY 2010

Impact Factor: 4.77 · DOI: 10.1021/jp9083184

CITATIONS
7

READS
30

5 AUTHORS, INCLUDING:

Ho-Jin Son
Korea University, Sejong, Korea
38 PUBLICATIONS **701** CITATIONS
SEE PROFILE

Won-Sik Han
Seoul Women's University
55 PUBLICATIONS **744** CITATIONS
SEE PROFILE

Available from: Ho-Jin Son
Retrieved on: 01 February 2016

Electrochemically Active Dendrimers for the Manufacture of Multilayer Films: Electrochemical Deposition or Polymerization Process by End-Capped Triarylamine or Carbazole Dendrimer

Ho-Jin Son,[†] Won-Sik Han,[†] Su Jung Han,[‡] Chongmok Lee,*[,‡] and Sang Ook Kang*[,†]

Department of Advanced Material Chemistry, Korea University, Sejong, Chungnam 339-700, South Korea, and Department of Chemistry and Nano Science, Ewha Womans University, Seoul 120-750, South Korea

Received: August 28, 2009; Revised Manuscript Received: October 24, 2009

Two different end-capped triarylamine and carbazole dendrimers of the types **G*n*-2^{n+1}NPB** and **G*n*-2^{n+1}CBP** ($n = 1, 2, 3, 4$) were prepared by divergent synthesis by reacting diethenyl propagating carbosilane dendrimers with suitable functional groups, such as naphthylphenylaminophenyl (NPB) and carbazolylphenyl (CBP) units. The electrochemical studies of these two series showed that the electrochemical properties of each dendrimer in both solution and on the immobilized electrode were dependent on the generation of dendrites and type of periphery group. **G*n*-2^{n+1}NPB** dendrimers ($n = 3, 4$) underwent oxidative precipitation on the electrode surface without a proceeding electrochemical reaction only to form highly charged ammonium cations, whereas the **G*n*-2^{n+1}CBP** dendrimers produced cross-linked polymers via an oxidative polymerization process. The ammonium cationic species of the **G3-16NPB** dendron was confirmed on the basis of the characteristic 1s peak of the F atom in X-ray photoelectron spectroscopy (XPS). Overall, the electrochemically activated **G3-16NPB** dendron transforms to a highly charged species with peripheral $NR_3^+BF_4^-$ units to undergo an electrodeposition (ED) process. As a result, the NPB and CBP dendrimers produce dissimilar deposited films, exhibiting different surface morphology and hydrophilicity based on atomic force microscope and contact angle measurements. Using these two dissimilar electrochemical deposition processes, a new method for fabricating multilayer thin films on a conducting substrate was demonstrated successfully.

Introduction

An electrode surface treatment using a conducting polymer has attracted considerable interest because the metal/organic interface is a critical issue affecting the performance of many organic semiconductor devices, including electrochromic windows and displays,[1,2] field effect transistors,[3] and photovoltaic cells.[4] Various methods have been proposed for efficient film fabrication, such as screen printing,[5] brush painting,[6] the wire-bar and doctor blade technique,[7,8] and inkjet printing.[9−11] In particular, spin-coating is a convenient, simple, and inexpensive method for manufacturing organic light emitting diodes (OLEDs).[12,13] However, in the preparation of multilayer devices, spin-coating has the disadvantage that it is a wet procedure that may partially dissolve preexisting layers. One approach used to protect the existing layers against interfacial erosion by the organic solvents used in the spin-casting of subsequent layers is to subject the existing layer to a posttreatment procedure, such as a cross-linking process based on photopolymerization driven by UV irradiation or thermal annealing. As other alternatives, electro-polymerization has received a great deal of attention due to its diverse merits, such as mass production, reproducibility, and ability to derive a homogeneous thickness distribution.[14,15] In most cases, electroactive monomers, such as thiophene,[16] pyrrole,[17−20] aniline,[21−27] and carbazole,[28−33] are essential for electro-polymerization. Electro-polymerization is generally initiated by electrochemical oxidation to produce stable, adherent, electrochemically active films on the electrodes. Indeed, several papers have reported the successful modification of metal electrodes using an electrochemical deposition method with their recent applications for OLED device.[35−55]

Recently, new types of electrodeposition processes based on a dendritic architecture were introduced with different deposition mechanisms. For example, polycationic organometallic redox-active dendrimers suggested the possibility of modifying the electrode surfaces for the fabrication of electrochemical biosensors and sensors for anions.[56,57] Similar to this finding, it was recently found that the rigid ethenyl-linked carbosilane dendrimers containing two different periphery groups, naphthylphenylaminophenyl (NPB) and carbazolylphenyl (CBP), exhibited novel electrochemical behavior, in which electrochemical deposition was controlled by the generation of dendrites.[58] Once electrochemically deposited, the dendrimer films remained intact in the depositing solvent. The second layer could then be fabricated without damaging the previous layer.

In an effort to gain further insight into the deposition mechanisms of multilayer stacking, this study examined the electrochemical process arising from electroactive group modified dendrons that would be significantly different depending on the peripheral groups. Indeed, there are two different deposition processes among the **G*n*-2^{n+1}NPB** and **G*n*-2^{n+1}CBP** dendrimer series. **G*n*-2^{n+1}NPB** dendrimers undergo a charge-induced deposition process as a result of the formation of cationic ammonium species. On the other hand, **G*n*-2^{n+1}CBP** dendrimers show typical electro-polymerization, i.e., cross-linking between the peripheral carbazole moieties. To examine the new dendritic deposition process observed in the NPB series, photophysical and surface analyses of the deposited **G3-16NPB**

* To whom correspondence should be addressed. Tel.: +82-41-860-1334. Fax: +82-41-867-5396. E-mail: cmlee@ewha.ac.kr (C.L.); sangok@korea.ac.kr (S.O.K.).
[†] Korea University.
[‡] Ewha Womans University.

10.1021/jp9083184 © 2010 American Chemical Society
Published on Web 12/29/2009

SCHEME 1: Synthetic Route for G*n*-2^{n+1}NPB

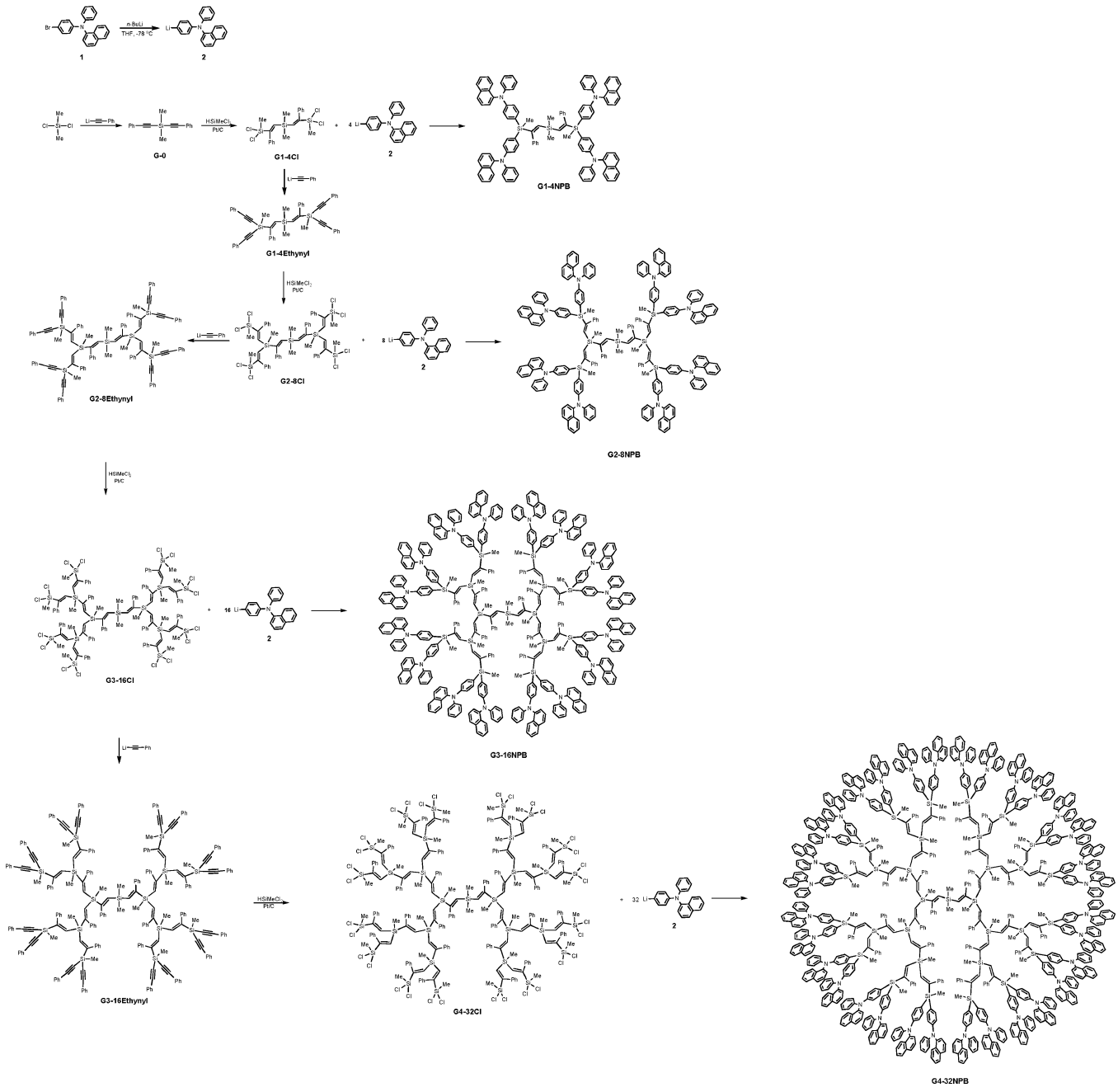

films were carried out to determine if the peripherial triarylamine groups had become quarternerized. The electrochemically deposited **G3-16NPB** films showed characteristic peaks at approximately 450−600 and 800 nm, indicating that a considerable part of the films consisted of the cationic form of [**G3-16NPB**$^{16+}$][PF^{6-}]$_{16}$. In addition, XPS revealed the existence of fluoride counteranions. With two different electrodeposition processes in hand, stepwise multilayer fabrication was demonstrated with **G*n*-2^{n+1}NPB** and **G*n*-2^{n+1}CBP**.

Experimental Section

General Procedures. All reactions were carried out under a dried N_2 atmosphere. Tetrahydrofuran (THF) was dried from sodium benzophenone ketyl. 1,4-Dibromobenzene, *N*-phenyl-1-naphthylamine, and carbazole were purchased from Aldrich and used without purification. Dichloromethylsilane was purchased from Gelest and used after vacuum distillation. A platinum catalyst (Pt on activated carbon, 10% Pt content) was purchased from Strem Chemicals and used after being vacuum-dried at room temperature. The ^{1}H and ^{13}C NMR spectra were recorded on a Varian Mercury 300 spectrometer operating at 300.1 and 75.44 MHz, respectively. Elemental analysis and MALDI mass spectroscopy (ABI Voyager STR) were performed at the Pusan and Daejon Branches of the Korean Basic Science Institute. The molecular weight distributions (M_w/M_n) were determined by gel permeation chromatography (GPC) using a Waters instrument equipped with Stragel HR 3, 4, and 5 columns.

Absorption and Fluorescence. UV−vis absorption spectra were recorded on a SHIMADZU UV-3101PC UV−vis−near-IR scanning spectrophotometer. The photoemission was examined using a VG ESCALAB 220i system with a hemispherical

SCHEME 2: Synthetic Route for G*n*-2^{n+1}CBP

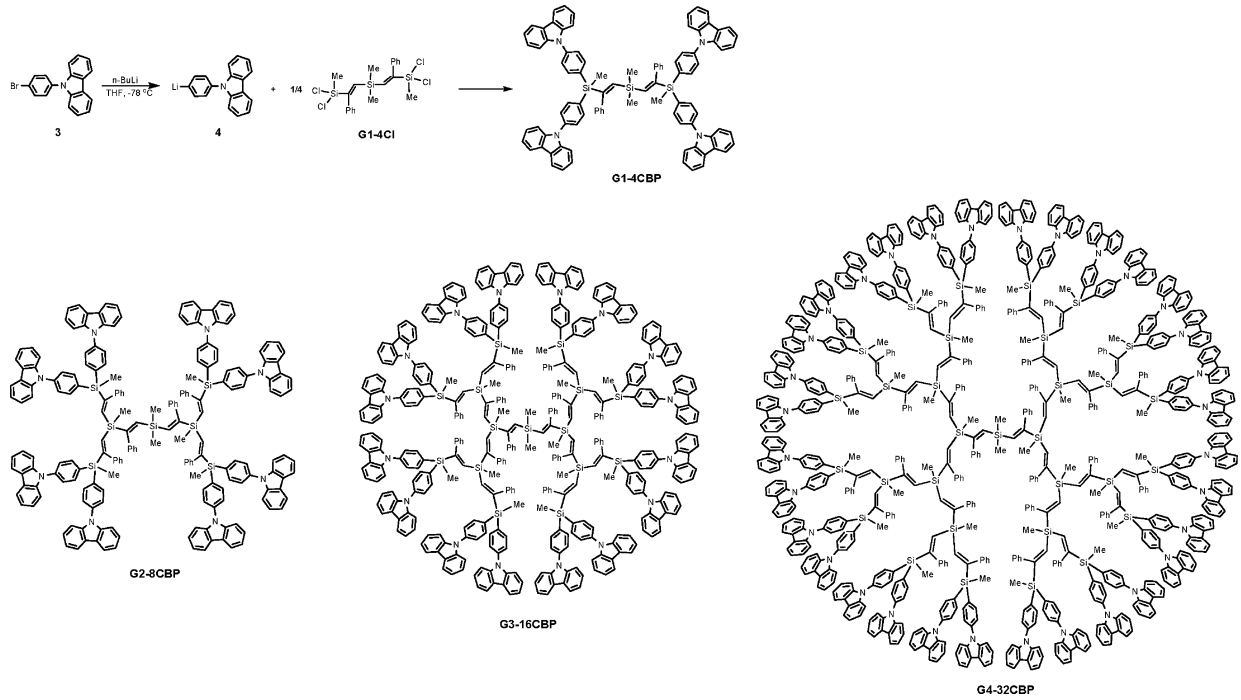

electron energy analyzer with magnesium source (1253.6 eV) as a light source. Contact angle (CA) measurements were performed using a Phoenix 300 goniometer (Surface Electro Optics Co., Ltd.).

AFM Image. Atomic force microscopy (AFM) images were measured at bare ITO and deposited film by electrodeposition in air and ambient conditions by contact mode and silicon contilever with spring constant 0.2 nN/m using a commercial AFM (Nanofocus Inc.). The cross-sectional image was examined by a field-emission scanning electron microscope (FE-SEM, Hitachi S4200).

Cyclic Voltammetry. The cyclic voltammetry experiments were performed using a BAS 100 electrochemical analyzer. The three-electrode cell system was used containing a platinum disk or ITO, a platinum wire, and $Ag/AgNO_3$ as the working, counter, and reference electrodes, respectively. Freshly distilled, degassed CH_2Cl_2 was used as the solvent with 0.1 M tetrabutylammonium tetrafluoroborate as the supporting electrolyte. The potential values were calibrated with respect to the $Fc^+|Fc$ (Fc = Ferrocene) redox couple. G*n*-type carbosilane dendrimers were obtained using the literature method.[59,60] The quantities of the surface coverage of the deposited film were determined by the coulometric assay from the areas encompassed by cyclic voltammograms.[61] The thickness of the dried film of both NPB and CBP dendrimers were ca. 0.3 μm for the surface coverage of 5.0×10^{-8} mol·cm^{-2}, which enables the calibration from the surface coverage to the thickness.

Results and Discussion

We first describe the electrochemical studies on two types of carbosilane dendrimers end-capped either by triarylamine or carbazole unit, showing that they undergo dissimilar oxidative precipitation processes on the surface of electrode by forming highly charged ammonium cations or cross-linked polymers, respectively. Such processes are not only controlled by the dendron generation but also dependent on solvent polarity. We then present photophysical properties, X-ray photoelectron spectra, and contact angle measurements as well as AFM measurements to provide the evidence that there exist two different electrodeposition processes depending on the peripheral end groups of carbosilane dendrimer.

Synthesis of G*n*-2^{n+1}NPB and G*n*-2^{n+1}CBP Dendrimers. NPB/CBP end-capped dendrimers (**G*n*-2^{n+1}NPB/-CBP**) of the first to fourth generation were produced via two-step synthesis in moderate yield of 48−63% (see the Supporting Information for details). A reaction of lithium-4-(*N*-phenyl-1-naphthylamino)phenyl (**2**) and lithium-4-(*N*-carbazolyl)phenyl (**4**) with the $SiCl_2$-terminated dendrimers **G*n*-2^{n+1}Cl** ($n = 1-4$) resulted in the production of the corresponding NPB/CBP-substituted dendrimers. Schemes 1 and 2 show the syntheses of the first to fourth generation NPB/CBP end-capped dendrimers along with a simplified drawing of each dendrimer. The white colored or gel type **G*n*-2^{n+1}NPB/-CBP** was obtained in pure form after simple column chromatography with CH_2Cl_2/hexane. In all cases, the terminal dichlorosilyl groups reacted completely with the lithium salt (**2** and **4**) to give dendrimers with monodisperse GPC traces and no residual dichloromethylsilyl resonances in their ^{1}H NMR spectra. The first-generation dendrimers were white solids, but the second- to fourth-generation dendrimers were hard gels. All generations showed good solubility in a wide range of organic solvents, including toluene, CH_2Cl_2, Et_2O,

TABLE 1: GPC and MALDI-TOF Mass Data

compounds	M_w	PDI	t_R (min)	MALDI-TOF mass data
G1-4NPB	1526.1	1.008	18.75	1527.88 $[M + H]^+$
G2-8NPB	3284.6	1.004	17.52	3285.10 $[M + H]^+$
G3-16NPB	6803.6	1.007	16.83	6823.51 $[M + Na]^+$
G4-32NPB	13835.6	1.011	16.15	13869.33 $[M + K]^+$
G1-4CBP	1317.8	1.007	18.87	1318.82 $[M + H]^+$, 1341.75 $[M + Na]^+$
G2-8CBP	2868.0	1.006	17.65	2868.98 $[M + H]^+$, 2892.13 $[M + Na]^+$, 2908.16 $[M + K]^+$
G3-16CBP	5968.4	1.001	16.90	5992.31 $[M + Na]^+$, 6007.65 $[M + K]^+$
G4-32CBP	12169.2	1.009	16.22	12192.93 $[M + Na]^+$

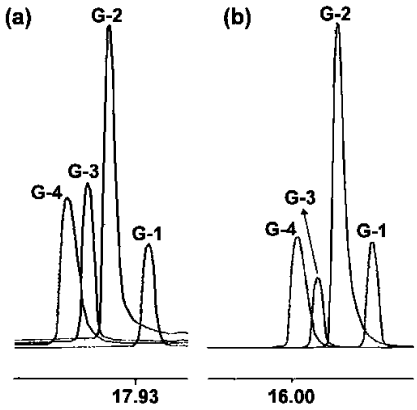

Figure 1. GPC data for **G*n*-2^{n+1}NPB** (a) and **G*n*-2^{n+1}CBP** (b).

and THF. **G*n*-2^{n+1}NPB/-CBP** were identified by NMR spectroscopy, size exclusion chromatography (SEC), cyclic voltammetry (CV), and elemental analysis. The MALDI-TOF mass spectra of the first generation show molecular ion peaks (m/z) that agreed well with the calculated values (see Table 1). The purity of the end-capped dendrimers was determined by SEC. The GPC data for each of the prepared end-capped dendrimers provided additional information on the unified characteristics of all generations. The polydispersity index (PDI) remained almost constant from the first to fourth generation (M_w/M_n = 1.001−1.011), indicating their pure dendritic properties with low PDI values. The regular decrease in retention time highlighted the distinctive difference in dendrimer size with increasing number of periphery groups (see Figure 1). The discrepancy between the theoretical and experimental molecular weights (relative to the polystyrene standards) was attributed to the difference between the hydrodynamic volumes of polystyrene as a standard and the prepared monodendrons.

Electrochemical Properties. The electrochemical properties of the two types of dendrimers, **G*n*-2^{n+1}NPB** and **G*n*-2^{n+1}CBP**, were examined by CV. To determine the deposition mechanism, third-generation dendrimers of the type **G3-16NPB** and **G3-16CBP** were taken as representative systems for each series, which showed maximized deposition and a sharp growth rate. As shown in Figure 2a,b, naphthylphenylaminophenyl end-capped **G3-16NPB** showed one reversible oxidation peak at 0.5 V, while carbazolylphenyl-modified **G3-16CBP** exhibited two quasi-reversible oxidation peaks at ∼0.5 and 0.7 V with respect to the $Fc^+|Fc$ couple. The peak current of the oxidative wave is proportional to the number of periphery groups. As shown in Figure 3a,b, an adherent film on the electrode surface was formed successfully from continuous cycling (100 mV/s) of the working electrode potential between − 0.25 and +1.2 V in the N_2-saturated CH_2Cl_2 solution containing the **G3-16NPB** and **G3-16CBP** dendrimers and Bu_4NBF_4. The electrodeposited films were almost transparent but had distinctive colors with **G3-16NPB** and **G3-16CBP** being purple and yellowish green, respectively. Parts c and d of Figure 3 show one and two diagnostic surface-immobilized CVs of **G3-16NPB** and **G3-16CBP**, respectively. There was a linear relationship of the peak currents depending on the potential scan rates of υ = 0.025, 0.05, and 0.1 V s^{-1}. They showed well-defined reversible surface redox waves in a fresh CH_2Cl_2/0.1 M Bu_4NBF_4 solution after successive potential sweep cycles with a surface coverage of $\Gamma = 2.8 \times 10^{-8}$ mol·cm^{-2} ($E_{1/2}$ = 0.49 V) and $\Gamma = 1.3 \times 10^{-8}$ mol·cm^{-2} ($E_{1/2}$ = 0.63 and 0.82 V) for **G3-16NPB** and **G3-16CBP**, respectively.

Different ED mechanisms appear to be operative based on the results from the successive potential scans at the oxidation potentials for each series, as shown in Figure 3a,b. In the case of **G3-16CBP**, the newly generated peaks increased with continuous potential scans, featuring a typical oxidative electropolymerization mechanism initiated by dimerization between the neighboring electroactive carbazole moieties (see Figure 3b). Similar electro-polymerization has been well-documented in other carbazole derivatives.[28−33] These oxidized peaks appeared at less positive potentials at around 0.6 V when compared to those of the parent phenylcarbazole unit at around 0.8 V. In contrast, such a shift was not pronounced for **G3-16NPB**. As shown in Figure 3a, only one broad reversible oxidation peak centered at 0.5 V increased with continuous cycles, suggesting a different deposition process. A comparison of the magnitude of surface coverage between these two series revealed a difference in coverage according to the dendrimer generations. Figure 4a clearly shows that effective deposition begins from the third generation of **G*n*-2^{n+1}NPB**. This can be explained by the assumptions that oxidized dendrons induce precipitation if the oxidized center remains in the ionic form even after continuous CV cycles. In addition, the observed electroprecipitation will be dominant when the number of such ionic centers increase with dendritic generation. Therefore, the solubility of the oxidized dendrimer is dependent on the number of charged peripheral groups, and effective deposition was observed in the third-generation dendrimer of **G3-16NPB**. A similar process has been reported in other dendritic structures containing with ferrocene units.[62] In the case of end-capped carbazole dendrim-

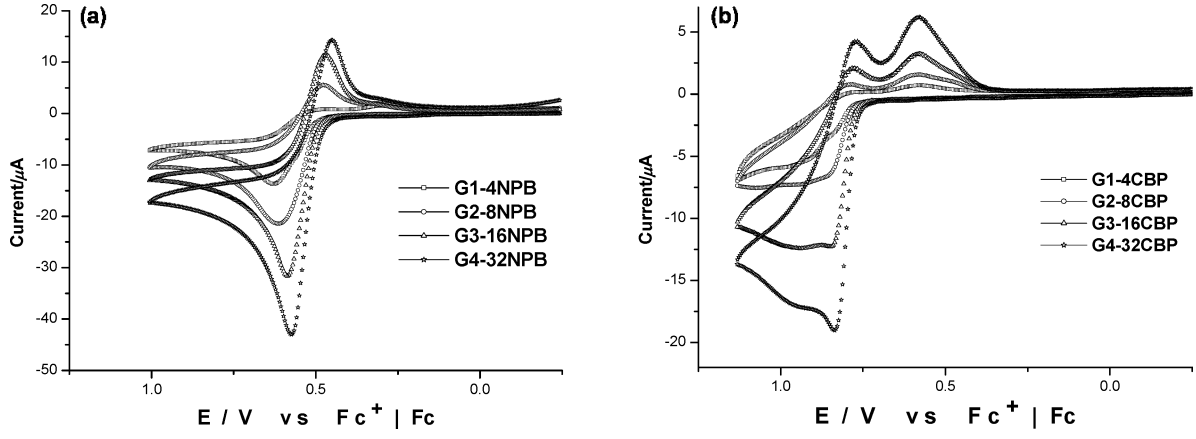

Figure 2. Change in the CVs depending on the generations of (a) 0.5 mM **G*n*-2^{n+1}NPB** and (b) 0.1 mM **G*n*-2^{n+1}CBP** in CH_2Cl_2 solution containing 0.1 M Bu_4NBF_4 on a Pt disk electrode (φ = 1.6 mm) with a scan rate (υ) of 0.1 V s^{-1}.

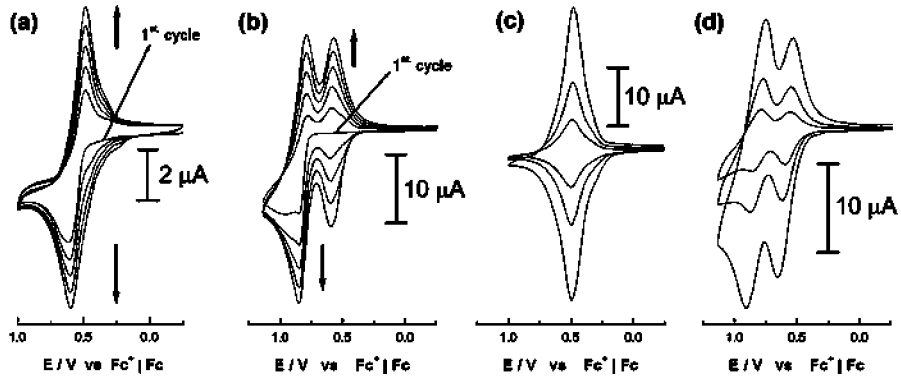

Figure 3. Change in the CVs on a Pt disk electrode (φ = 1.6 mm) containing 0.06 mM (a) **G3-16NPB** and (b) **G3-16CBP** in a 0.1 M Bu_4NBF_4/CH_2Cl_2 solution with scan rate (υ) of 0.1 V s^{-1} for five cycles, and CVs of a Pt disk electrode (φ = 1.6 mm) modified with (c) **G3-16NPB** (Γ = 2.8 × 10^{-8} mol·cm^{-2}) and (d) **G3-16CBP** (Γ = 1.3 × 10^{-8} mol·cm^{-2}) in Bu_4NBF_4/CH_2Cl_2 with υ = 0.025, 0.05, and 0.1 V s^{-1} (from inside to outside), respectively.

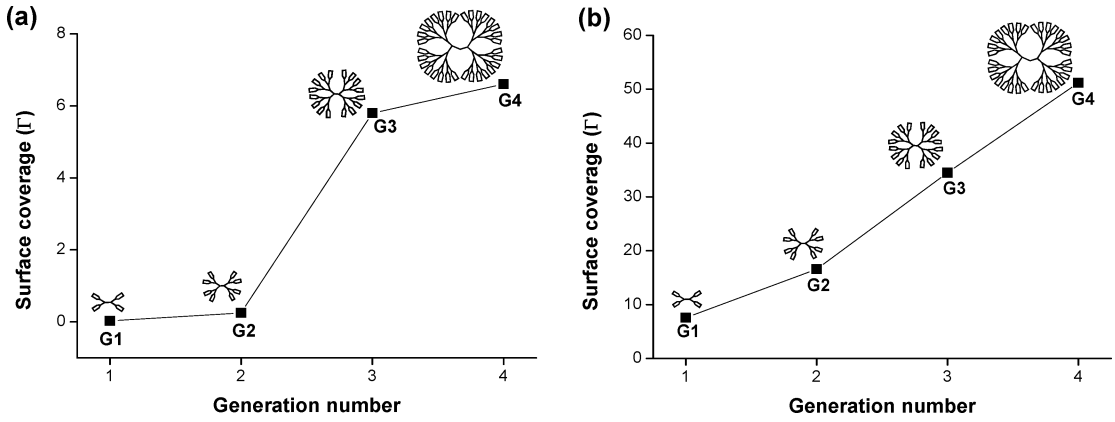

Figure 4. Surface coverage (Γ/(10^{-9} mol·cm^{-2})) of ITO modified with a film deposited in a CH_2Cl_2 solution containing (a) 0.5 mM **G*n*-2^{n+1}NPB** and (b) 0.1 mM **G*n*-2^{n+1}CBP**/0.1 M Bu_4NBF_4 with at a scan rate (υ) of 0.1 V s^{-1} for five cycles.

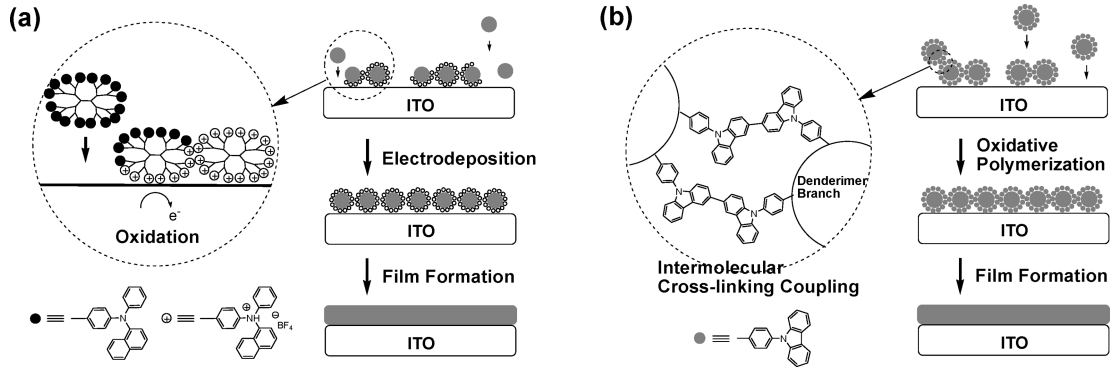

Figure 5. Electrodeposition mechanism of (a) NPB dendrimer and (b) CBP dendrimer.

ers, deposition began even in the first generation of **G1-4CBP**, confirming electro-polymerization between neighboring carbazole units (see Figure 4b).

To obtain further information on sequential film formation and the resulting film stability, an exfoliation experiment on the two preformed **G3-16NPB/-CBP** ED films was carried out in both CH_2Cl_2 and CH_3CN solvent. As shown in Figure 6, two ED films did not show any exfoliation phenomenon in the CH_2Cl_2 solution containing only a supporting electrolyte as a result of the low solubility of the highly oxidized **G3-16NPB** and cross-linked **G3-16CBP**. However, when exfoliation was performed in a more polar CH_3CN solution, the charged forms of **G3-16NPB** were removed easily from its ED film, suggesting surface dissociation of the ED film through the dissolution of ammonium salt in polar media (see Figure 7a). Indeed, in the cyclic voltammetry cell, broken pieces were observed during continuous cycling for the exfoliation test of the **G3-16NPB** ED film. On the other hand, the CVs of the **G3-16CBP** ED film was maintained stably with increasing cycle numbers without a decrease in peak current (Figure 7b). From the exfoliation experiments, **G3-16NPB** appeared to proceed through a charge-enhanced deposition mechanism, as proposed in Figure 5a. The oxidative stability due to the presence of a pendant naphthalene unit at the naphthylphenylaminophenyl group blocked the electro-polymerization process. Figure 5b shows electro-polymerization process by oxidative coupling between the electroactive 3- and 6-positions of the carbazole units in the **G*n*-2^{n+1}CBP** series.

Photophysical Study (UV and PL) and Electrochromism at a Positive Potential. Two ED films were investigated further by examining their optical properties. Figures 8 and 9 show

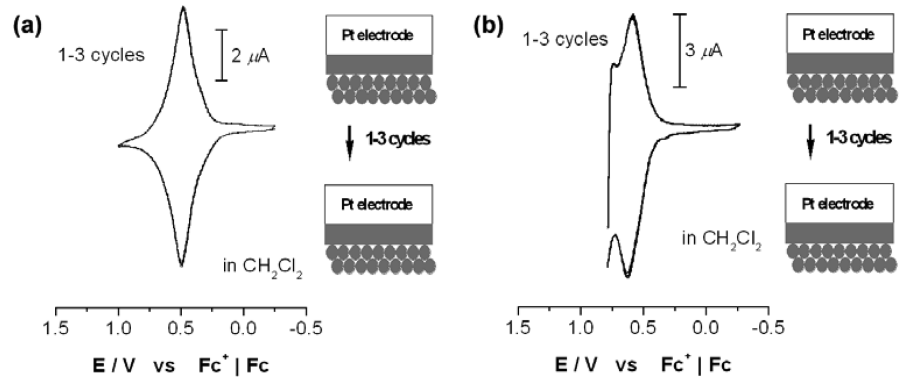

Figure 6. CVs and scheme of (a) **G3-16NPB** and (b) **G3-16CBP** film-modified Pt electrode in CH_2Cl_2 solution containing 0.1 M Bu_4NBF_4 after holding the electrode potential at 1.0 V for 100 s.

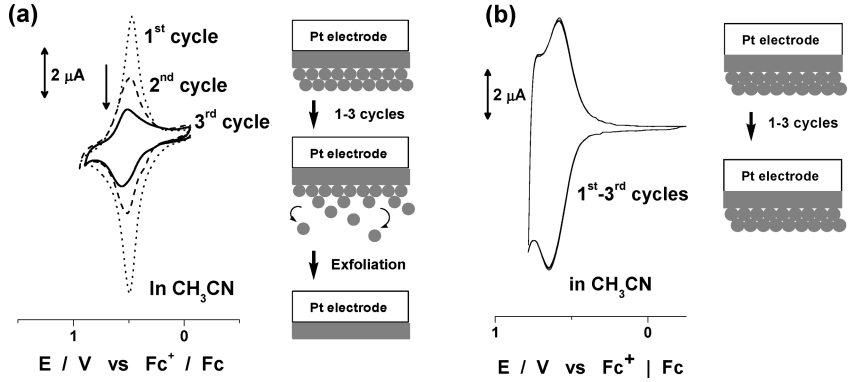

Figure 7. CVs and schematic diagram of (a) **G3-16NPB** and (b) **G3-16CBP** film-modified Pt electrode in CH_3CN solution containing 0.1 M Bu_4NBF_4 after holding the electrode potential at 1.0 V for 100 s.

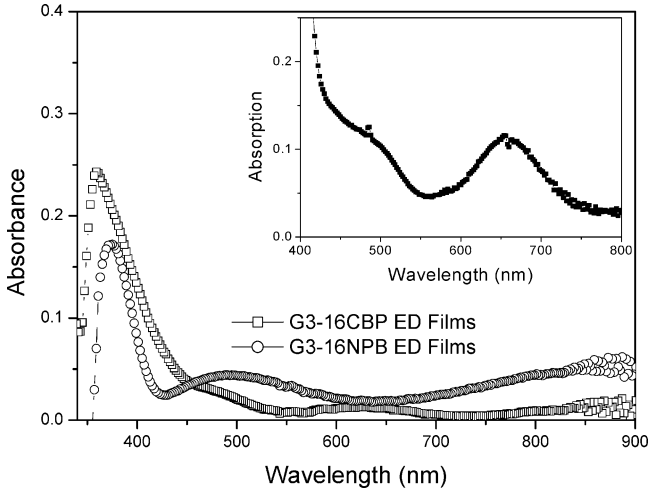

Figure 8. UV−visible spectra of a film of **G3-16NPB** (circles) and **G3-16CBP** (squares) electrodeposited onto an ITO electrode. Inset: The UV−visible spectra of the **G3-16CBP** ED film recorded after the film was oxidized at 0.70 V.

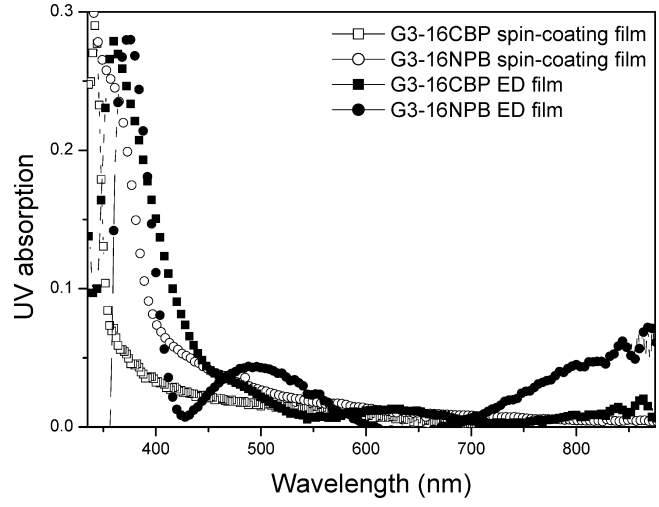

Figure 9. UV−visible spectra of a film of **G3-16NPB** (triangles) and **G3-16CBP** (circles) spin-coated (opend) and electrodeposited (closed) onto an ITO electrode.

the UV−vis absorption spectra of the ED films of **G3-16NPB** and **G3-16CBP** on ITO, along with those of the spin-coated films for comparison. The spin-coated films exhibited two absorption peaks at 292 and 349 nm, respectively, which were attributed to the $\pi \rightarrow \pi^*$ transition from carbazole and *N*-phenyl-1-naphtylamino phenyl periphery groups. For the ED films of **G3-16CBP**, the absorption peaks of the $\pi-\pi^*$ transition were red-shifted by 8 nm compared to the corresponding spin-coated films as a result of extended π-conjugation by cross-linking between the periphery phenyl carbazole units. The broad tail band ranging from 600 to 900 nm was also observed clearly. This low-energy band was observed in other carbazole-based ED films and is believed to be related to the dications of dimeric carbazole.[63] Although this broad tail band in these ED films is relatively lower than that reported in other carbazole-based ED films, it suggests that cationic dimeric carbazole exists in the ED films. This is consistent with the CV observations, which showed less positive dimeric peaks due to cross-linking between two neighboring dendrimers. On the other hand, the ED films of **G3-16NPB** exhibited new absorption bands in the visible region along with a slightly red-shifted $\pi \rightarrow \pi^*$ transition centered at $\lambda_{max} = 374$ nm. New peaks consisting of two distinctive regions were observed, one at around 450 and 600 and the other

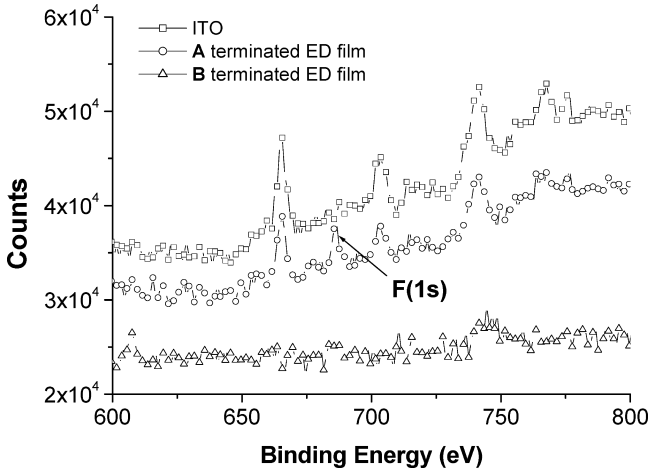

Figure 10. XPS spectra of ITO and **G3-16NPB** (A) and **G3-16CBP** (B) ED films.

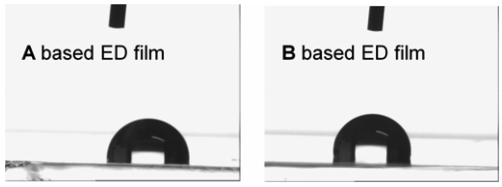

Figure 11. Photographs of the water droplet shape on (left) **G3-16NPB** (A) based ED film with a CA of 85.7 ± 0.9° and (right) **G3-16CBP** (B) based ED film with a CA of 96.5 ± 1.5°.

at approximately 800 and 900 nm. These new absorptions were attributed to the formation of aminyl radical cations, and a similar peak pattern was identified in triarylamines.[64−69]

X-ray Photoelectron Spectra and Contact Angle Measurements. XPS was performed to obtain information on the aminyl radical cation species in the ED films of **G3-16NPB**. For comparison, a bare ITO film was also prepared with two ED films. Figure 10 shows the XPS spectra of the three films prepared. The peak at around 680 eV corresponds to the spin−orbit line of the 1s electrons of the fluorine atom.[70] As shown in Figure 10, one fluorine peak at 685 eV was observed in the ED films of **G3-16NPB**, indicating the existence of the counteranion, BF_4^-. This suggests that the reduced ED films of **G3-16NPB** contain ammonium salts with its counteranion, BF_4^-, even after electrochemical deposition. No discernible peak was observed at a similar energy in the case of the ED films of **G3-16CBP**. Such spectral analysis of the ED films of **G3-16NPB** and **G3-16CBP** confirmed that each dendron proceeds through two different ED mechanisms, either charge-enhanced precipitation or polymerization.

The surface hydrophilicity of the two ED films prepared was also evaluated by water CA measurements. As shown in Figure 11, the CA values for the ED films of **G3-16NPB** and **G3-16CBP** were 85.7 ± 0.9 and 96.5 ± 1.5°, respectively. This suggests that the ED films of **G3-16NPB** are more hydrophilic than those of **G3-16CBP** due to the presence of radical cation species remaining in the ED films of **G3-16NPB**. Considering that the hydrophobic dendrimer branch units dictate a large part of each dendron, even such a small difference in CA between the two series supports the charged states of the ED films of **G3-16NPB**.

Stepwise Double-Layer Film Formation by the Application of Electrochemical Process with G3-16NPB and G3-16CBP. In an attempt to demonstrate successful film formation and examine the morphological properties of the resulting films, **G3-16NPB** and **G3-16CBP** were deposited electrochemically and sequentially onto an ITO electrode. Figure 12a shows the results of cycling the potential between −0.3 and 1.2 V vs $Fc^+|Fc$ applied to an ITO electrode in a mixed CH_2Cl_2 solution containing 0.5 mM **G3-16NPB/G3-16CBP** and 0.1 M Bu_4NBF_4. From the end of the five cycles, the deposition of **G3-16NPB,** whose reversible voltammetric wave was obtained, showed the accumulation of the insoluble polycationic form of **G3-16NPB** on the ITO surface (see red dot line (**A**) in Figure 12a). The ED film of **G3-16NPB** was insoluble in CH_2Cl_2. Subsequently, the second cycling of 100 mV/s, followed by the transfer of the thoroughly washed electrode to fresh 0.1 M Bu_4NBF_4/CH_2Cl_2 containing **G3-16CBP**, produced well-defined voltammetric waves for the accumulated polymeric film, designated the ITO/**G3-16NPB** ED film/**G3-16CBP** ED film (see blue solid line (**B**) in Figure 12a). Figure 12b shows a representative scheme of this electrochemical deposition. Figure 12b also shows an image of the ED films of **G3-16NPB** onto the ITO electrode before (up) and after (down) modification with **G3-16CBP**. Prior to modification, distinctive circular dots were observed over the entire image and are thought to be related to the presence of independent highly charged polycationic species. This may be due to much less cross-linking ability of the peripheral NPB unit of the **G3-16NPB** dendrimer. Such appearance corroborates well with previous studies on redox-active ferrocenyl dendrimers.[71] In contrast, after the second deposition, the surface appeared to be essentially featureless, showing a film morphology smoothed by the intermolecular cross-linking of **G3-16CBP**.

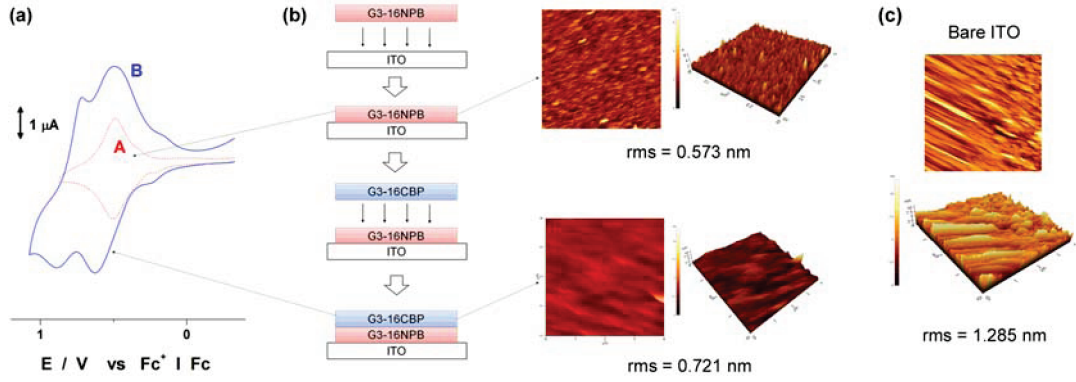

Figure 12. (a) CVs for a successively electrodeposited **G3-16NPB** and **G3-16CBP** on a Pt electrode in a CH_2Cl_2 solution containing 0.1 M Bu_4NBF_4: (A) after **G3-16NPB** deposition but before **G3-16CBP** deposition (red dotted line); (B) after successive **G3-16CBP** deposition (blue solid line). (b) AFM images of the deposited **G3-16NPB** and **G3-16CBP** film on an ITO electrode. (c) Bare ITO surface for comparison.

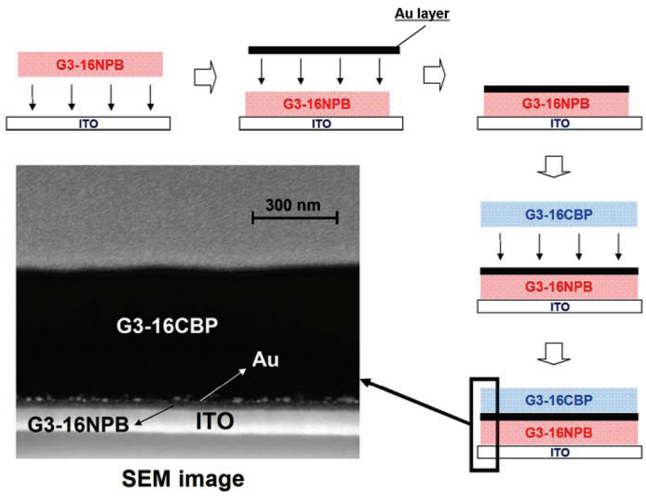

Figure 13. Representative scheme for fabricating the **G3-16NPB**/Au/**G3-16CBP** three-layered film and its cross-sectional SEM image.

In addition, to confirming the successive formation of a double layer, a pretreatment was carried out by sputtering Au onto the preformed **G3-16NPB** ED film, where Au was used as an indicator to easily discriminate between the two ED films. Figure 13 shows a representative cross-sectional scanning electron microscopy (SEM) image of the three-layer structure (ITO/**G3-16NPB** ED film/Au/**G3-16CBP** ED film). Compared to the two ED films, the relatively bright spots of Au play the role of a borderline indicator as well. These experimental data clearly show that multilayer structures can be fabricated by applying successive electrochemical processes using suitable dendrimer precursors.

Conclusions

New ED processes were developed employing a simple CV technique on dendrimers containing electrochemically active peripheral groups, such as **G*n*-2^{n+1}NPB** and **G*n*-2^{n+1}CBP**. Upon continuous potential scans in the CV experiments, arylamine functionalized dendrons of the type, **G*n*-2^{n+1}NPB**, showed their ED process to be significantly dependent on the number of highly charged radical cationic species, reaching maximum efficiency in the case of **G3-16NPB**. UV−vis absorption and XPS spectra provided direct evidence of the formation of radical cationic species. On the basis of subsequent exfoliation experiments, it was confirmed that the once-deposited oxidized form of **G3-16NPB** was easily exfoliated in polar solvents by applying a reverse electrochemical reduction process. A distinctive electro-polymerization process was evident when the end-capped carbazole dendron of the type **G3-16CBP** was oxidized, yielding nonreversible cross-linked carbazole oligomers and polymers. The stepwise formation of multiple layers was demonstrated by the application of successive electrochemical processes with **G3-16NPB** being the first followed by **G3-16CBP**. Fabrication of OLEDs using this method along with device optimization is in progress.

Acknowledgment. This work was supported by a grant (F0004010-2008-31) from Information Display R&D Center, one of the Knowledge Economy Frontier R&D Programs funded by the Ministry of Knowledge Economy of Korean government, and the Korea Research Foundation Grant funded by the Korean Government (MOEHRD, Basic Research Promotion Fund, Grant KRF-2008-314-C00186).

Supporting Information Available: Experimental details including synthesis, ^{1}H and ^{13}C NMR spectroscopic data, and MALDI-TOF mass spectroscopic data as well as PL data. This material is available free of charge via the Internet at http://pubs.acs.org.

References and Notes

(1) Gaupp, C. L.; Welsh, D. M.; Rauh, R. D.; Reynolds, J. R. *Chem. Mater.* **2002**, *14*, 3964.
(2) Argun, A. A.; Aubert, P. H.; Thompson, B. C.; Schwendeman, I.; Gaupp, C. L.; Hwang, J.; Pinto, N. J.; Tanner, D. B.; MacDiarmid, A. G.; Reynolds, J. R. *Chem. Mater.* **2004**, *16*, 4401.
(3) Sirringhaus, H.; Brown, P. J.; Friend, R. H.; Nielsen, M. M.; Bechgaard, K.; Langveld-Voss, B. M. W.; Spiering, A. J. H.; Janssen, R. A. J.; Meijer, E. W.; Herwig, P.; de Leeuw, D. M. *Nature* **1999**, *401*, 685.
(4) Granstrom, M.; Petritsch, K.; Arias, A. C.; Lux, A.; Andersson, M. R.; Friend, R. H. *Nature* **1998**, *395*, 257.
(5) Shaheen, S. E.; Radspinner, R.; Peyghambarian, N.; Jabbour, G. E. *Appl. Phys. Lett.* **2001**, *79*, 2996.
(6) Kim, S. S.; Na, S. I.; Jo, J.; Tae, G.; Kim, D. Y. *Adv. Mater.* **2007**, *19*, 4410.
(7) Ouyang, J.; Guo, T. F.; Yang, Y.; Higuchi, H.; Yoshioka, M.; Nagatsuka, T. *Adv. Mater.* **2002**, *14*, 915.
(8) Tseng, S. R.; Meng, H. F.; Lee, K. C.; Horng, S. F. *Appl. Phys. Lett.* **2008**, *93*, 153308.
(9) Sirringhaus, H.; Kawase, T.; Friend, R. H.; Shimoda, T.; Inbasekaran, M.; Wu, W.; Woo, E. P. *Science* **2000**, *290*, 2133.
(10) Sirringhaus, H.; Kawase, T.; Friend, R. H. *Mater. Res. Bull.* **2001**, *26*, 539.
(11) Bharathan, J.; Yang, Y. *Appl. Phys. Lett.* **1998**, *72*, 2660.
(12) Kraft, A.; Grimsdale, A. C.; Holmes, A. B. *Angew. Chem., Int. Ed.* **1998**, *37*, 402.
(13) Burroughes, J. H.; Bradley, D. D. C.; Brown, A. R.; Marks, R. N.; Mackay, K.; Friend, R. H.; Burn, P. L.; Holmes, A. B. *Nature* **1990**, *347*, 539.
(14) Cui, C. Q.; Ong, L. H.; Tan, T. C.; Lee, J. Y. *Electrochim. Acta* **1993**, *38*, 1395.
(15) Dahlaus, M.; Beck, F. *J. Appl. Electrochem.* **1993**, *23*, 957.
(16) Roncali, J. *Chem. Rev.* **1992**, *92*, 711.
(17) Cross, M. G.; Walton, D.; Morse, N. J.; Mortimer, R. J.; Rosseinsky, D. R.; Simmonds, D. J. *J. Electroanal. Chem.* **1985**, *189*, 389.
(18) Haase, V.; Beck, F. *Electrochim. Acta* **1994**, *39*, 1195.
(19) Tsuchiya, M.; Matsui, S.; Sano, K.; Kojima, T. *J. Appl. Polym. Sci.* **1998**, *70*, 471.
(20) Sadki, S.; Schottland, P.; Brodie, N.; Sabouraud, G. *Chem. Soc. Rev.* **2000**, *29*, 283.
(21) Pei, Q.; Bi, X. *J. Polym. Sci.* **1989**, *38*, 1819.
(22) Chen, S. A.; Feng, W. G. *Macromolecules* **1991**, *24*, 1242.
(23) Dogan, S.; Akbulut, U.; Toppaie, L. *Synth. Met.* **1992**, *53*, 19.
(24) Sherman, B. C.; Euler, W. B.; Ren, F. R. *J. Chem. Educ.* **1994**, *71* (4), A94.
(25) Yang, J.; Zhao, C.; Cui, D.; Hou, J.; Wan, M.; Xu, M. *J. Appl. Polym. Sci.* **1995**, *56*, 831.
(26) Sari, B.; Talu, M. *Synth. Met.* **1998**, *94*, 221.
(27) Li, X. G.; Huang, M. R.; Duan, W. *Chem. Rev.* **2002**, *102*, 2925.
(28) Ambrose, J. F.; Nelson, R. F. *J. Electrochem. Soc.* **1968**, *115*, 1159.
(29) Ambrose, J. F.; Carpenter, L. L.; Nelson, R. F. *J. Electrochem. Soc.* **1975**, *122*, 876.
(30) Morin, J. F.; Leclerc, M.; Ade, D.; Siove, A. *Macromol. Rapid Commun.* **2005**, *26*, 761.
(31) Taranekar, P.; Fulghum, T.; Patton, D.; Ponnapati, R.; Clyde, G.; Advincula, R. C. *J. Am. Chem. Soc.* **2007**, *129*, 12537.
(32) Baba, A.; Onishi, K.; Knoll, W.; Advincula, R. C. *J. Phys. Chem. B* **2004**, *108*, 18949.
(33) Desbene-Monvernay, A.; Lacaze, P. C.; Delamar, M. *J. Electroanal. Chem.* **1992**, *334*, 241.
(34) Abruna, H. D.; Denisevich, P.; Umana, M.; Meyer, T. J.; Murray, R. W. *J. Am. Chem. Soc.* **1981**, *103*, 1.
(35) Linford, R. G., Ed. *Electrochemical Science and Technology of Polymers*; Elsevier: London and New York, 1987.
(36) Skotheim, T. A., Ed. *Handbook of Conducting Polymers*; Dekker: New York, 1986; Vols. 1 and 2.
(37) Deronzier, A.; Moutet, J. C. *Acc. Chem. Res.* **1989**, *22*, 249.
(38) Heinze, J. *Top. Curr. Chem.* **1990**, *152*, 1.
(39) Merz, A. *Top. Curr. Chem.* **1990**, *152*, 49.
(40) Curran, D.; Grimshaw, J.; Perera, S. D. *Chem. Soc. Rev.* **1991**, *20*, 391.
(41) Murray, R. W., Ed. *Molecular Design of Electrode Surfaces*; Wiley Interscience: New York, 1992.

(42) Novak, P.; Müller, K.; Santhanam, K. S. V.; Hass, O. *Chem. Rev.* **1997**, *97*, 207.
(43) McQuade, D. T.; Pullen, A. E.; Swager, T. M. *Chem. Rev.* **2000**, *100*, 2537.
(44) Roncali, J.; Blanchard, P.; Frere, P. *J. Mater. Chem.* **2005**, *15*, 1589.
(45) Cosnier, S. *Handb. Biosens. Biochips* **2007**, *1*, 237.
(46) Tang, S.; Liu, M.; Gu, C.; Zhao, Y.; Lu, P.; Lu, D.; Liu, L.; Shen, F.; Yang, B.; Ma, Y. *J. Org. Chem.* **2008**, *73*, 4212.
(47) Chiang, C. C.; Chen, H. C.; Lee, C. S.; Leung, M. K.; Lin, K. R.; Hsieh, K. H. *Chem. Mater.* **2008**, *20*, 540.
(48) Chang, C. C.; Leung, M. K. *Chem. Mater.* **2008**, *20*, 5816.
(49) Lin, K. R.; Chien, Y. H. C.; Chang, C. C.; Hsieh, K. H.; Leung, M. K. *Macromolecules* **2008**, *41*, 4158.
(50) Fulghum, T. M.; Taranekar, P.; Advincula, R. C. *Macromolecules* **2008**, *41*, 5681.
(51) Li, M.; Tang, S.; Shen, F.; Liu, M.; Xie, W.; Xia, H.; Liu, L.; Tian, L.; Xie, Z.; Lu, P.; Handif, M.; Lu, D.; Cheng, G.; Ma, Y. *J. Phys. Chem. B* **2006**, *110*, 17784.
(52) Taranekar, P.; Huang, C.; Fulghum, T. M.; Baba, A.; Jiang, G.; Park, J.-Y.; Advincula, R. C. *Adv. Funct. Mater.* **2008**, *18*, 347.
(53) Jegadesan, S.; Sindhu, S.; Advincula, R. C.; Valiyaveettil, S. *Langmuir* **2006**, *22*, 780.
(54) Jagadesan, S.; Advincula, R. C.; Valiyaveettil, S. *Adv. Mater.* **2005**, *17*, 1282.
(55) Inaoka, S.; Roitman, D. B.; Advincula, R. C. *Chem. Mater.* **2005**, *17*, 6781.
(56) Casado, C. M.; Cuadrado, I.; Moran, M.; Alonso, B.; Garcia, B.; Gonzalez, B.; Losada, J. *Coord. Chem. Rev.* **1999**, *185*−*186*, 53.
(57) Takada, K.; Diaz, D. J.; Abruna, H. D.; Cuadrado, I.; Gonzalez, B.; Casado, C. M.; Alonso, B.; Moran, M.; Losada, J. *Chem.*−*Eur. J.* **2001**, *7*, 1109.
(58) Son, H. J.; Han, W. S.; Lee, K. H.; Jung, H. J.; Lee, C.; Ko, J.; Kang, S. O. *Chem. Mater.* **2006**, *18*, 5811.
(59) Kim, C.; Kim, M. *J. Organomet. Chem.* **1998**, *563*, 43.
(60) Son, H. J.; Han, W. S.; Kim, H.; Kim, C.; Ko, J.; Lee, C.; Kang, S. O. *Oraganometallics* **2006**, *25*, 766.
(61) Lee, C.; Anson, F. C. *Anal. Chem.* **1992**, *64*, 528.
(62) Alonso, B.; Moran, M.; Casado, C. M.; Lobete, F.; Lasada, J.; Cuadrado, I. *Chem. Mater.* **1995**, *7*, 1440.
(63) Li, M.; Shen, F.; Liu, M.; Xie, W.; Xia, H.; Liu, L.; Tian, L.; Xie, Z.; Lu, P.; Hanif, M.; Lu, D.; Cheng, G.; Ma, Y. *Chem. Commun. (Cambridge)* **2006**, 3393.
(64) Chou, M. Y.; Leung, M. K.; Su, Y. O.; Chiang, C. L.; Lin, C. C.; Liu, J. H.; Kuo, C. K.; Mou, C.-Y. *Chem. Mater.* **2004**, *16*, 654.
(65) Nelsen, S. F.; Pladziewicz, J. R. *Acc. Chem. Res.* **2002**, *35*, 247.
(66) Lambert, C.; Noll, G. *Chem.*−*Eur. J.* **2002**, *8*, 3467.
(67) Lambert, C.; Noll, G. *Angew. Chem., Int. Ed.* **1998**, *37*, 2107.
(68) Lambert, C.; Noll, G. *J. Am. Chem. Soc.* **1999**, *121*, 8434.
(69) Hauck, S. I.; Lakshmi, K. V.; Hartwig, J. F. *Org. Lett.* **1999**, *1*, 2057.
(70) Yang, W.; Auciello, O.; Butler, J. E.; Cai, W.; Carlisle, J. A.; Gerbi, J.; Gruen, D. M.; Knickerbocker, T.; Lasseter, T. L.; Russell, J. N., Jr.; Smith, L. M.; Hamers, R. J. *Nat. Mater.* **2002**, *1*, 253.
(71) Takada, K.; Diaz, D. J.; Abruna, H. D.; Cuadrado, I.; Casado, C.; Alonso, B.; Moran, M.; Losada, J. *J. Am. Chem. Soc.* **1997**, *119*, 10763.

JP9083184